Supporting Information

Tandem Aldol Reaction from Acetal Mixtures by an Artificial Enzyme with Site-Isolated Acid and Base Functionality

Ishani Bose and Yan Zhao*

Department of Chemistry, Iowa State University, Ames, Iowa 50011-3111, USA

**Corresponding author: zhaoy@iastate.edu*

Table of Contents

Syntheses

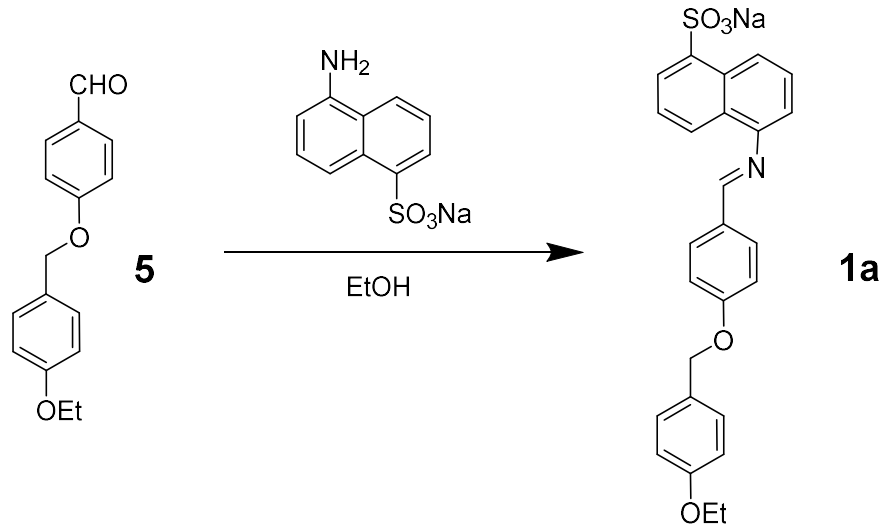

Scheme S1. Synthesis of Compound **1a**

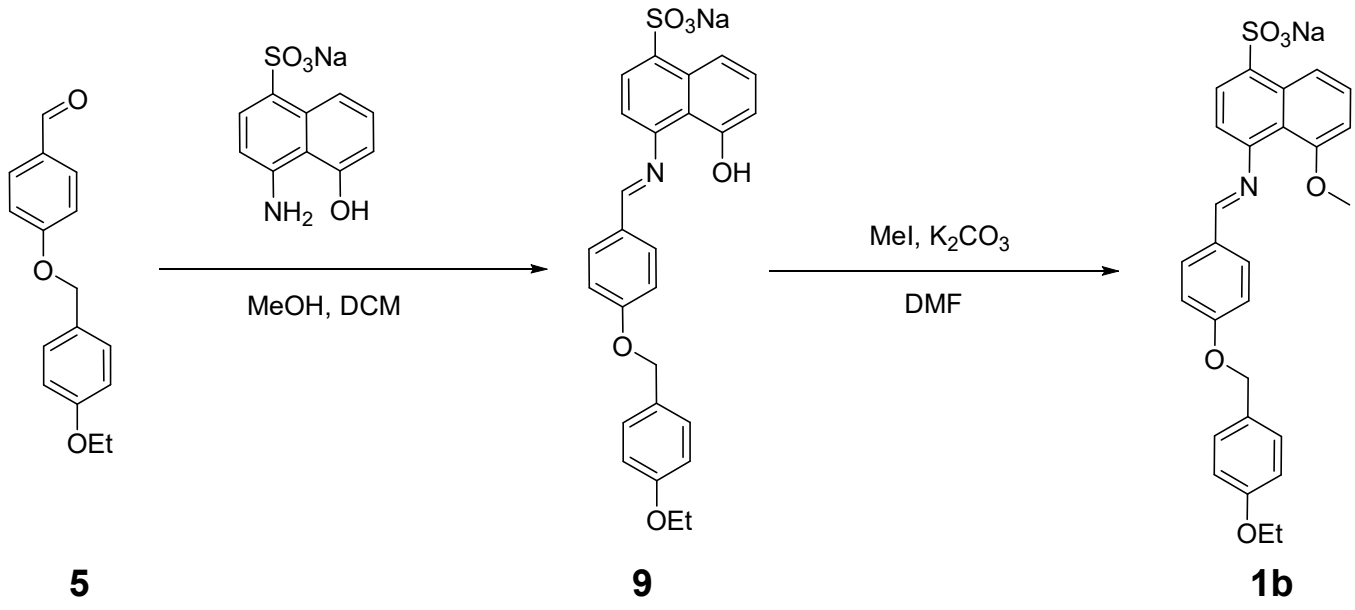

Scheme S2. Synthesis of Compound **1b**

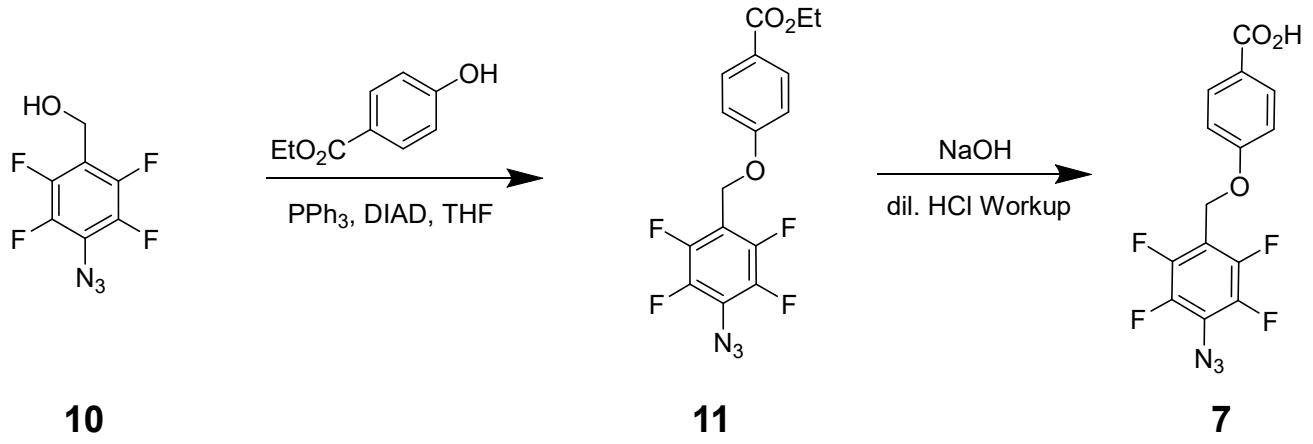

10 **11** **7**

Scheme S3. Synthesis of Compound **7**

Syntheses of compounds **2-4**,[1] **5**,[2] **8a**,[3] **8b/8e-i,**[4] **8c**,[5] and **10**[6] followed previously reported procedures.

Compound 1a. Compound **5** (0.10 g, 0.39 mmol, 1.0 equiv.) and sodium 5-aminonaphthalene-1-sulfonate (0.096 g, 0.39 mmol, 1.0 equiv.) were dissolved in 20 mL of ethanol. The reaction mixture was heated to reflux overnight. The reaction mixture was cooled to room temperature and diethyl ether (80 mL) was added slowly. The precipitate formed was collected by filtration and washed twice with 5 mL of diethyl ether to yield a brown powder (0.17 g, 90%). The product was used in the MINP preparation without further purification. ^{1}H NMR (400 MHz, 298 K, DMSO-d_6, δ): 8.71 (d, J = 8.4 Hz, 1H), 8.62 (s, 1H), 8.31 (d, J = 8.4 Hz, 1H), 8.07–7.99 (m, 3H), 7.52–7.40 (m, 4H), 7.19–7.16 (m, 3H), 6.95 (d, J = 8.4 Hz, 2H), 5.13 (s, 2H), 4.04 (q, J = 7.2, 6.8 Hz, 2H), 1.33 (t, J = 6.8 Hz, 3H). ^{13}C NMR (100 MHz, 298 K, DMSO-d_6, δ): 161.2, 159.9, 158.4, 148.4, 144.0, 130.7, 129.7, 129.6, 129.2, 129.1, 128.4, 125.8, 125.3, 124.9, 124.8, 124.1, 115.2, 114.3, 112.6, 69.3, 63.0, 14.6 ppm. HRMS (ESI) m/z: $[M - H]^-$ calcd for $C_{26}H_{23}NO_5S$, 460.1224; found 460.1203.

Compound 9. Compound **5** (0.10 g, 0.39 mmol, 1.0 equiv.) and sodium 4-amino-5-hydroxynaphthalene-1-sulfonate (0.10 g, 0.39 mmol, 1.0 equiv.) were dissolved in 20 mL of dry methanol and 2 mL of dry DCM. The reaction mixture was heated to reflux overnight. The reaction mixture was cooled to room temperature and diethyl ether (80 mL) was added slowly. The precipitate formed was collected by

filtration and washed twice with 5 mL of diethyl ether to yield a black powder (0.18 g, 92%). ^{1}H NMR (400 MHz, 298 K, CD_3OD, δ): 8.30 (d, J = 8.4 Hz, 1H), 7.97 (d, J = 8.0 Hz, 1H), 7.58 (d, J = 8.4 Hz, 2H), 7.43 (t, J = 8.0 Hz, 1H), 7.36 (d, J = 8.4 Hz, 2H), 7.06 (d, J = 8.4 Hz, 2H), 6.91 (d, J = 8.8 Hz, 2H), 6.82 (d, J = 7.2 Hz, 1H), 6.59 (d, J = 7.6 Hz, 1H), 5.77 (s, 1H), 5.05 (s, 2H), 4.04 (q, J = 6.8, 7.2 Hz, 2H), 1.39 (t, J = 6.8 Hz, 3H). ^{13}C NMR (100 MHz, 298 K, CD_3OD, δ): 161.5, 161.3, 160.2, 154.0, 145.5, 132.1, 131.7, 130.9, 130.3, 130.0, 128.9, 128.8, 128.7, 120.4, 115.9, 115.4, 109.3, 104.5, 86.4, 70.9, 64.5, 15.2 ppm. HRMS (ESI) m/z: $[M - H]^-$ calcd for $C_{26}H_{23}NO_6S$, 476.1173; found 476.1170.

Compound 1b. Compound **9** (50.0 mg, 0.10 mmol, 1.0 equiv.), methyl iodide (21.3 mg, 0.15 mmol, 1.5 equiv.) and K_2CO_3 (27.7 mg, 0.20 mmol, 2.0 equiv.) were mixed in 10 mL of dry DMF. The reaction mixture was stirred at room temperature overnight. Diethyl ether (40 mL) was added slowly. The precipitate formed was collected by filtration and washed twice with 5 mL of diethyl ether before purified on a short column to yield a brown powder (41.0 mg, 79%). The product was used in the MINP preparation without further purification. ^{1}H NMR (600 MHz, 298 K, CD_3OD, δ): 8.45 (d, J = 9.0 Hz, 1H), 8.35 (d, J = 9 Hz, 1H), 8.30 (d, J = 10.2 Hz, 1H), 8.03 (d, J = 9.0 Hz, 1H), 7.58 (d, J = 7.8 Hz, 1H), 7.48-7.43 (m, 1H), 7.40-7.38 (m, 1H), 7.07 (d, J = 7.2 Hz, 1H), 7.00 (d, J = 10.2 Hz, 1H), 6.94-6.88 (m, 1H), 6.83 (d, J = 8.4 Hz, 1H), 6.60 (d, J = 9.6 Hz, 1H), 6.31 (d, J = 9.6 Hz, 1H), 5.78 (s, 1H), 4.04 (q, J = 5.4, 8.4 Hz, 2H), 3.98 (s, 3H), 1.39 (t, J = 7.2 Hz, 3H). ^{13}C NMR (100 MHz, 298 K, CD_3OD, δ): 164.9, 161.4, 160.2, 159.4, 151.6, 141.4, 133.4, 131.3, 130.8, 129.9, 127.5, 124.1, 120.6, 120.0, 115.4, 110.8, 107.5, 105.5, 100.8, 64.5, 56.4, 36.9, 15.2 ppm. HRMS (ESI) m/z: $[M - H]^-$ calcd for $C_{27}H_{25}NO_6S$, 490.1330; found 490.1305.

Compound 11. Compound **10** (146.4 mg, 0.66 mmol, 1.1 equiv.) and ethyl 4-hydroxybenzoate (100.0 mg, 0.60 mmol, 1.0 equiv.) were added to a solution of diisopropyl azodicarboxylate (DIAD) (0.13 mL, 0.66 mmol, 1.1 equiv.) and PPh_3 (173.62 mg, 0.66 mmol, 1.1 equiv.) in 20 mL dry THF at 0 °C. After

being stirred at room temperature overnight, the reaction mixture was concentrated by rotary evaporation. The residue was purified by column chromatography over silica gel using 3:1 hexanes/ethyl acetate as the eluent to give a yellow powder (115.5 mg, 52%). ^{1}H NMR (400 MHz, 298 K, $CDCl_3$, δ): 8.01 (d, J = 8.8 Hz, 2H), 6.98 (d, J = 8.8 Hz, 2H), 5.10 (s, 2H), 4.34 (q, J = 7.2, 14.4 Hz, 2H), 1.38 (t, J = 7.2 Hz, 3H). ^{13}C NMR (100 MHz, 298 K, $CDCl_3$, δ): 166.4, 162.0, 147.1, 144.7, 137.7, 135.3, 131.7, 127.5, 123.8, 114.5, 101.4, 60.9, 57.9, 14.5 ppm. ^{19}F NMR (544 MHz, 298 K, $CDCl_3$, δ): 145.8, 161.9. HRMS (ESI) m/z: $[M + H]^+$ calcd for $C_{16}H_{11}F_4N_3O_3$, 370.0809; found 370.0819.

Compound 7. Aqueous NaOH (21.7 mg, 0.54 mmol, 2.0 equiv.) was added to a stirred solution of compound **11** (100.0 mg, 0.27 mmol, 1.0 equiv.) in 20 mL of 1:1 THF/EtOH mixture. The reaction mixture was heated to reflux overnight and then cooled to room temperature. After the organic solvents were removed by rotary evaporation, the residue was diluted with water, cooled to 0 °C, and made acidic with 6 N HCl. The mixture was extracted with ethyl acetate (3 × 20 mL) and the combined organic layer was concentrated by rotary evaporation. The residue was purified over silica gel using 1:1 n-hexane/ethyl acetate as the eluent to give a yellow powder (84.0 mg, 91%). ^{1}H NMR (600 MHz, 298 K, CD_3OD, δ): 7.90 (d, J = 8.4 Hz, 2H), 6.84 (d, J = 8.4 Hz, 2H), 4.88 (s, 2H). ^{13}C NMR (150 MHz, 298 K, CD_3OD, δ): 172.3, 170.1, 167.6, 163.3, 132.9, 122.7, 121.8, 116.2, 116.0, 20.6 ppm. ^{19}F NMR (376 MHz, 298 K, $CDCl_3$, δ): 138.8, 146.6. HRMS (ESI) m/z: $[M - H]^-$ calcd for $C_{14}H_7F_4N_3O_3$, 340.0351; found 340.0398.

^{1}H NMR spectra for MINP Preparation

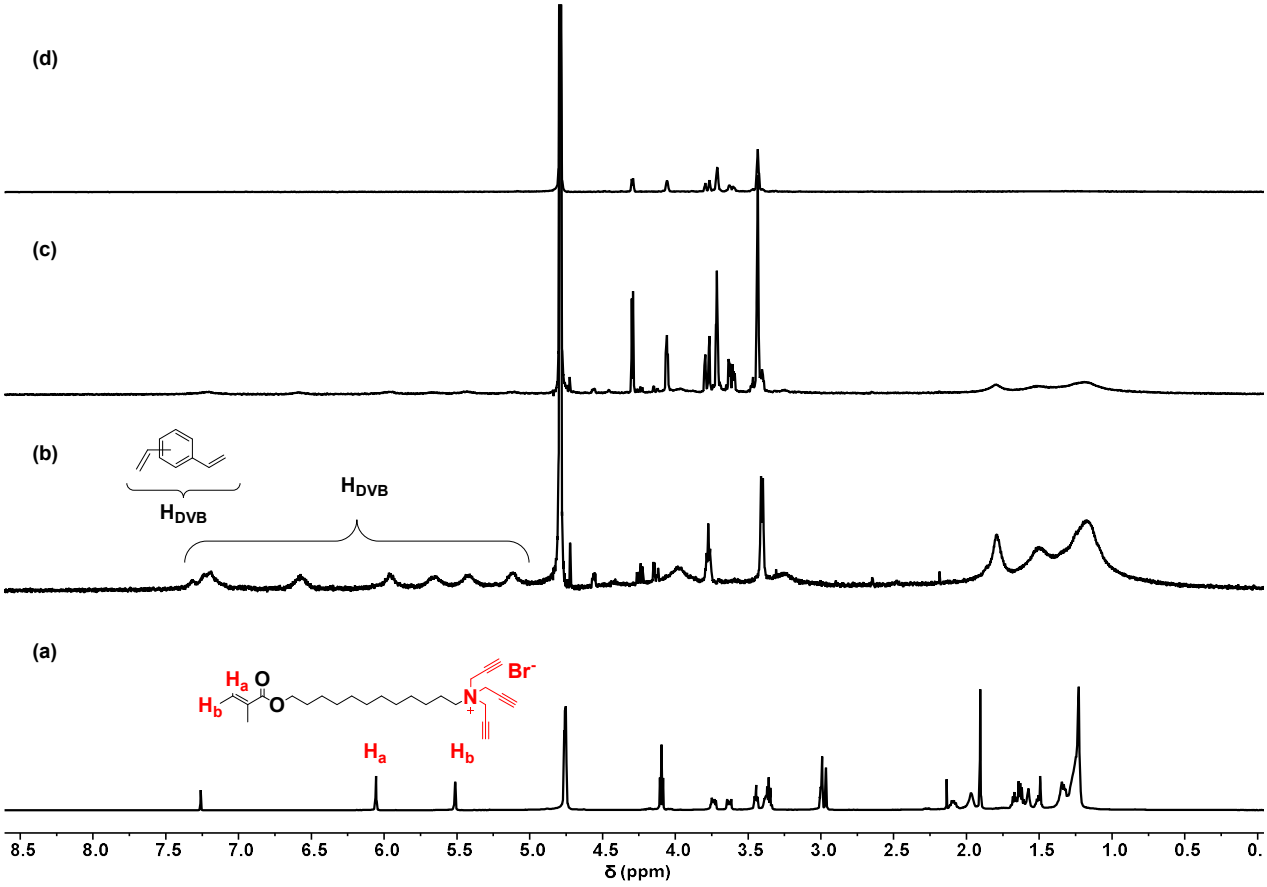

Figure S1. Stacked ^{1}H NMR spectra of (a) surfactant **2** in $CDCl_3$, (b) typical alkynyl surface cross-linked micelle in D_2O, (c) typical surface functionalized micelle in D_2O, (d) typical final MINP(**1a**+**7**) in D_2O.

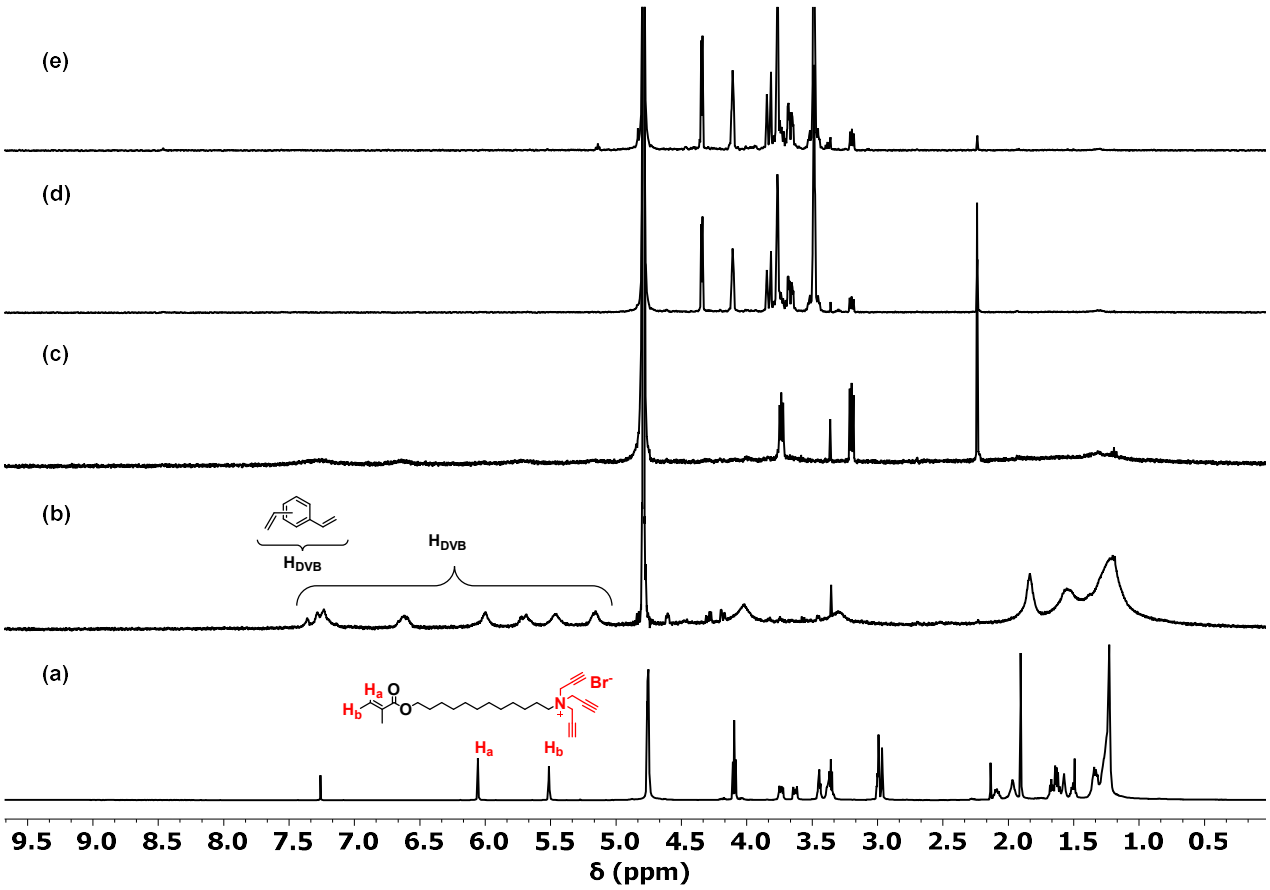

Figure S2. ^{1}H NMR spectra of (a) surfactant **2** in $CDCl_3$, (b) typical alkynyl surface cross-linked micelle in D_2O, (c) typical surface-functionalized micelle with 2-azidoethylamine in D_2O, (d) typical surface-functionalized micelle with **4** in D_2O, and (e) typical MINP(**1b**+**7**) after washing and re-dissolving in D_2O.

Dynamic Light Scattering

The particle size of MINP was determined on a Malvern Zetasizer Nano ZS using the Zetasizer software according to the Stokes-Einstein equation (S1). The volume of a spherical nanoparticle (V_{D_h}) was calculated from equation (S2). Assuming a density of 1.37 g/cm^3 (the density of protein), the molecular weight of the particle can be calculated using equation (S3).[7] A nanoparticle with a hydrodynamic diameter of 4.87 nm has a calculated molecular weight of 50 kDa, which was used in the calculation of the concentration.

$$D_h = \frac{k_B T}{6\pi\eta D_t} \qquad \text{(S1)}$$

in which D_h is the hydrodynamic diameter, D_t the translational diffusion coefficient measured by dynamic light scattering, T the temperature, k_B the Boltzmann's constant, and η is dynamic viscosity of water (0.890 cP at 298 K).

$$V_{D_h} = \frac{4\pi}{3}\left(\frac{D_h}{2}\right)^3 \qquad \text{(S2)}$$

$$\text{Mw in dalton} = \left(\frac{D_h}{0.132}\right)^3 \qquad \text{(S3)}$$

in which D_h is the hydrodynamic diameter in nm.

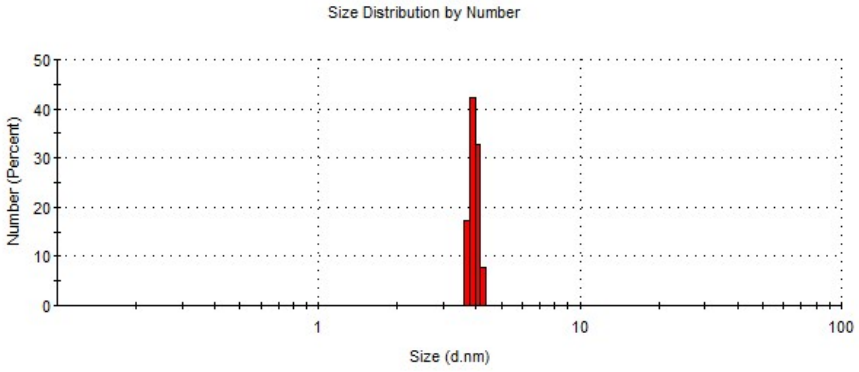

Figure S3. Distribution of the hydrodynamic diameters of the nanoparticles in water as determined by DLS for alkynyl-SCM (surface-cross-linked micelle). D = 3.94 ± 0.15 nm.

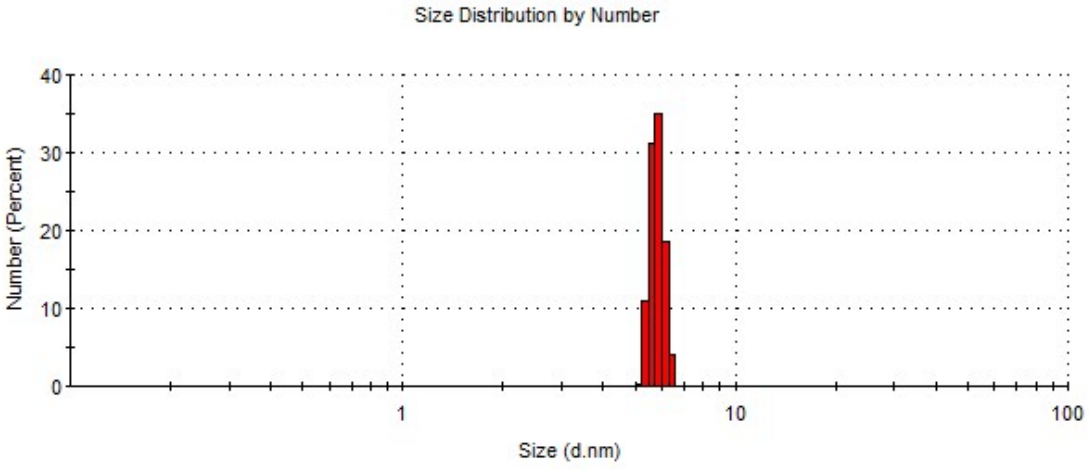

Figure S4. Distribution of the hydrodynamic diameters of the nanoparticles in water as determined by DLS for surface functionalized SCM (surface-cross-linked micelle). D = 5.87 ± 0.22 nm.

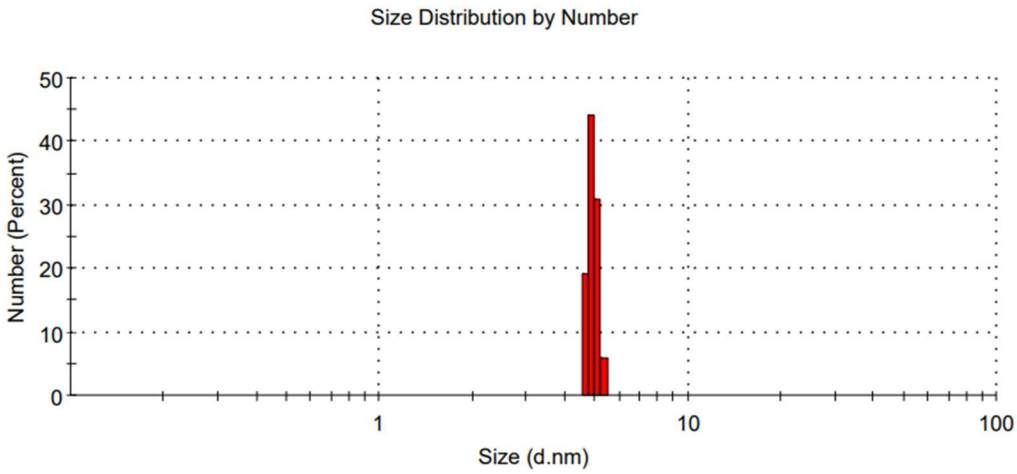

Figure S5. Distribution of the hydrodynamic diameters of the nanoparticles in water as determined by DLS for typical MINP(**1**+**7**). D = 4.94 ± 0.19 nm.

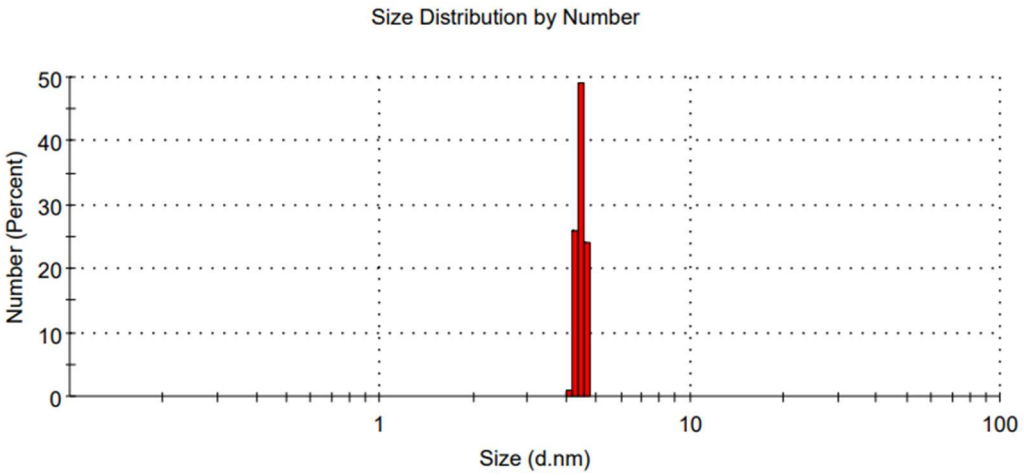

Figure S6. Distribution of the hydrodynamic diameters of the nanoparticles in water as determined by DLS for NH_2-MINP(**1b**+**7**). D = 4.45 ± 0.15 nm.

Transmission electron microscopy

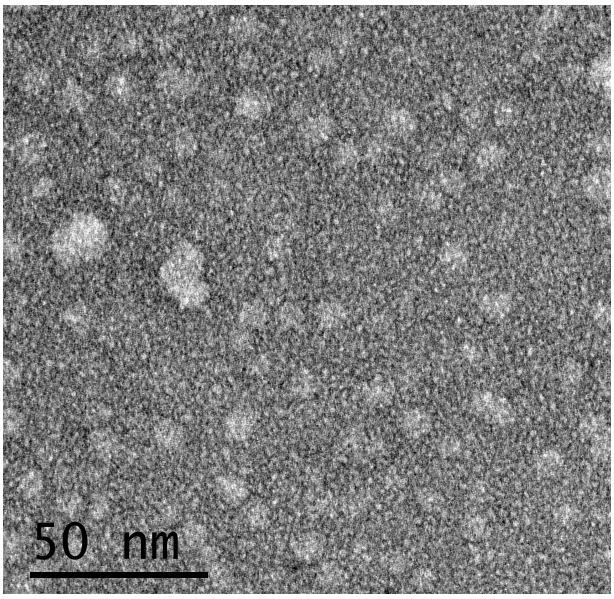

Figure S7. TEM image of typical MINPs (scale bar = 50 nm). For the TEM imaging, 0.1 mg of MINP was dissolved in 1 mL of Millipore water and the solution was ultra-sonicated for 10 min. A micro syringe was used to load one small drop (~1 μL) of the above solution onto a TEM copper grid covered with carbon film. The sample was left to form a thin layer, and then one small drop (~1 μL) of 2% uranyl acetate solution was loaded on the grid for the negative staining. The sample was left to dry and analyzed on a 200kV JEOL 2100 scanning/transmission electron microscope (STEM).

Hydrolysis Study

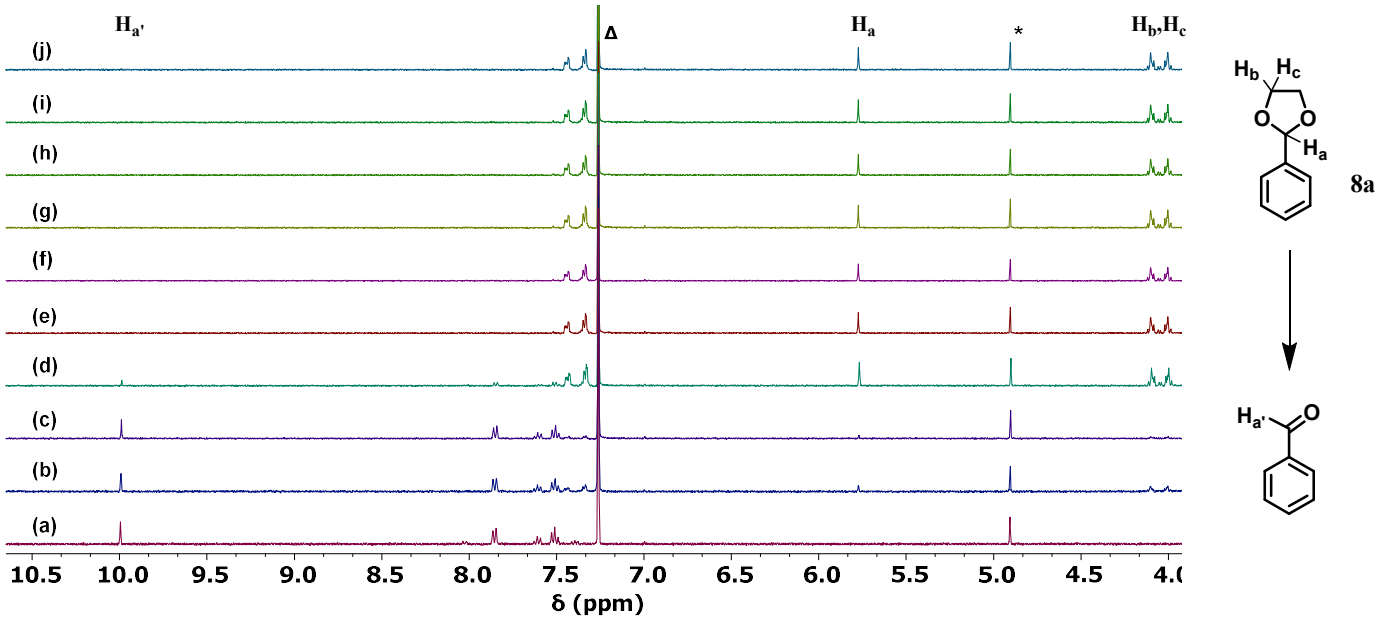

Figure S8. Partial ^{1}H NMR spectra of the hydrolyzed product from **8a** catalyzed by: (a) MINP(**1a**+**7**) (0.5 equiv. DVB), (b) MINP(**1a**+**7**) (0 equiv. DVB), (c) MINP(**1a**+**7**) (1 equiv. DVB), (d) MINP(**1a**)+**7** (0.5 equiv. DVB), (e) MINP(**1a**) (0.5 equiv. DVB), (f) **7**, (g) NINP (+ **7**) (0.5 equiv. DVB), (h) NINP + **7** (0.5 equiv. DVB, without radiation), (i) NINP (0.5 equiv. DVB), and (j) none. *: internal standard. Δ: $CHCl_3$. The data correspond to entries 1–10, respectively, in Table 1.

Hydrolysis of 8a–i in D_2O catalyzed by MINP catalysts

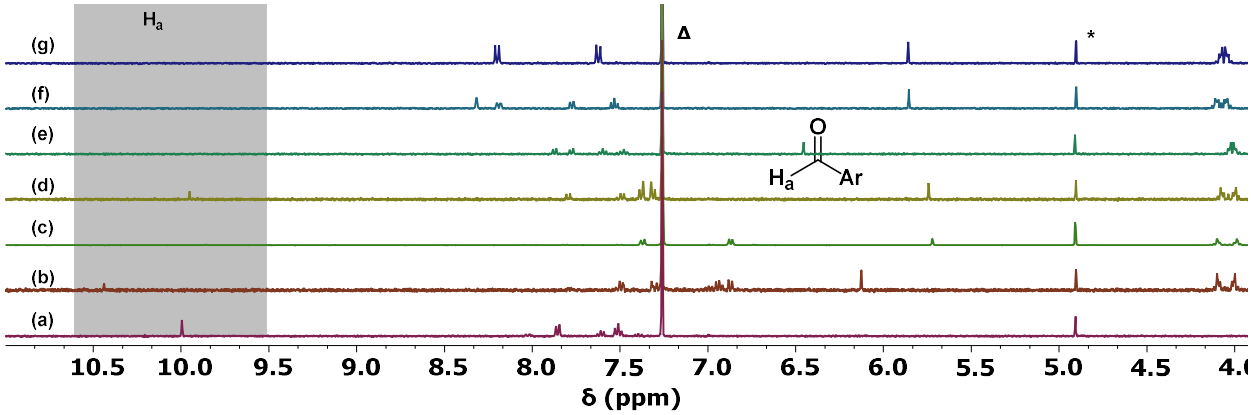

Figure S9. Partial ^{1}H NMR spectra of the hydrolyzed product by MINP(**1a**+**7**) from: (a) **8a**, (b) **8b**, (c) **8e**, (d) **8f**, (e) **8g**, (f) **8h**, and (g) **8i**. *: internal standard. Δ: $CHCl_3$. The data correspond to the appropriate entries in Table 2.

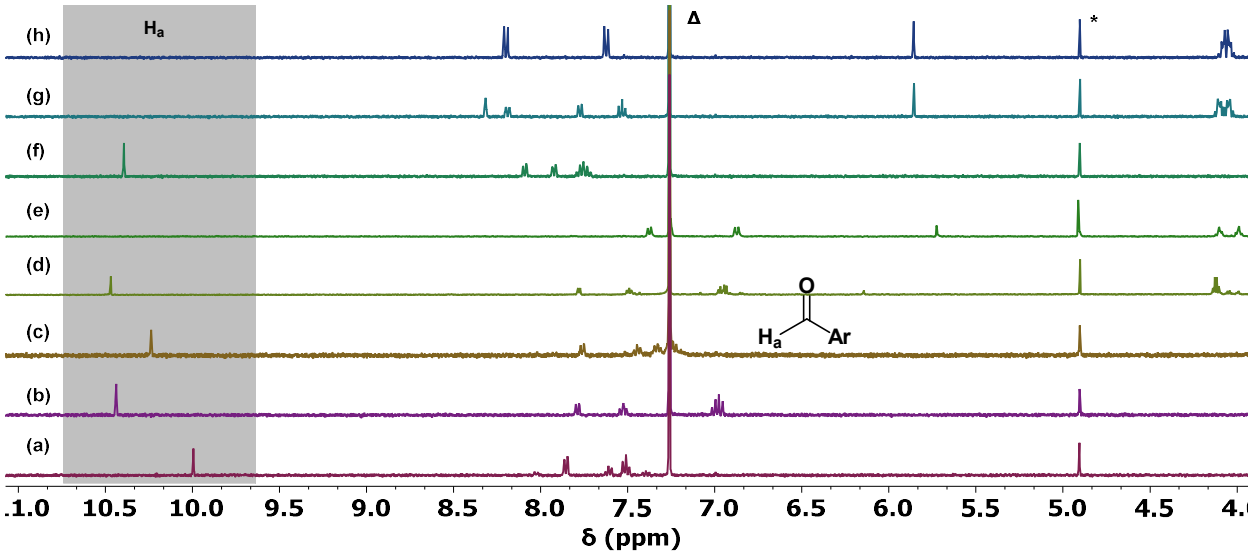

Figure S10. Partial ^{1}H NMR spectra of the hydrolyzed product by MINP(**1b**+**7**) from: (a) **8a**, (b) **8b**, (c) **8c**, (d) **8d**, (e) **8e**, (f) **8g**, (g) **8h**, and (h) **8i**. *: internal standard. Δ: $CHCl_3$. The data correspond to the appropriate entries in Table 2.

Hydrolysis of 8g as a function of solution pH

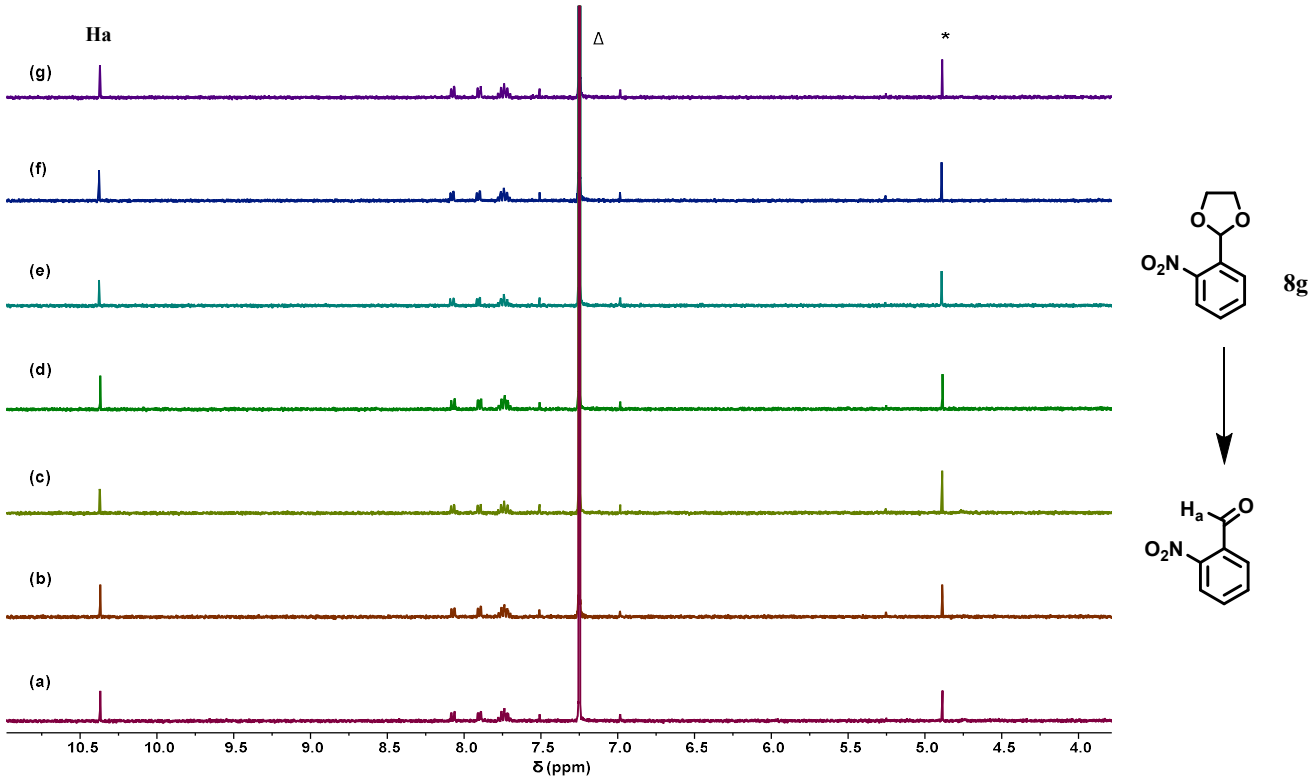

Figure S11. Partial ^{1}H NMR spectra of the hydrolyzed product of **8g** after 6 h at 50 °C catalyzed by: (a) MINP(**1b**+**7**) at pH 5, (b) MINP(**1b**+**7**) at pH 6, (c) MINP(**1b**+**7**) at pH 7, (d) MINP(**1b**+**7**) at pH 8, (e) MINP(**1b**+**7**) at pH 9, (f) MINP(**1b**+**7**) at pH 10, (g) MINP(**1b**+**7**) at pH 11. [10 mM buffer, pH = 5.0 acetate; 6.0 MES, 7.0–8.0 HEPES, 9.0 Tris, 10.0–11.0 CAPS buffer]. *: internal standard. Δ: $CHCl_3$. The data correspond to the appropriate entries in Figure 2b.

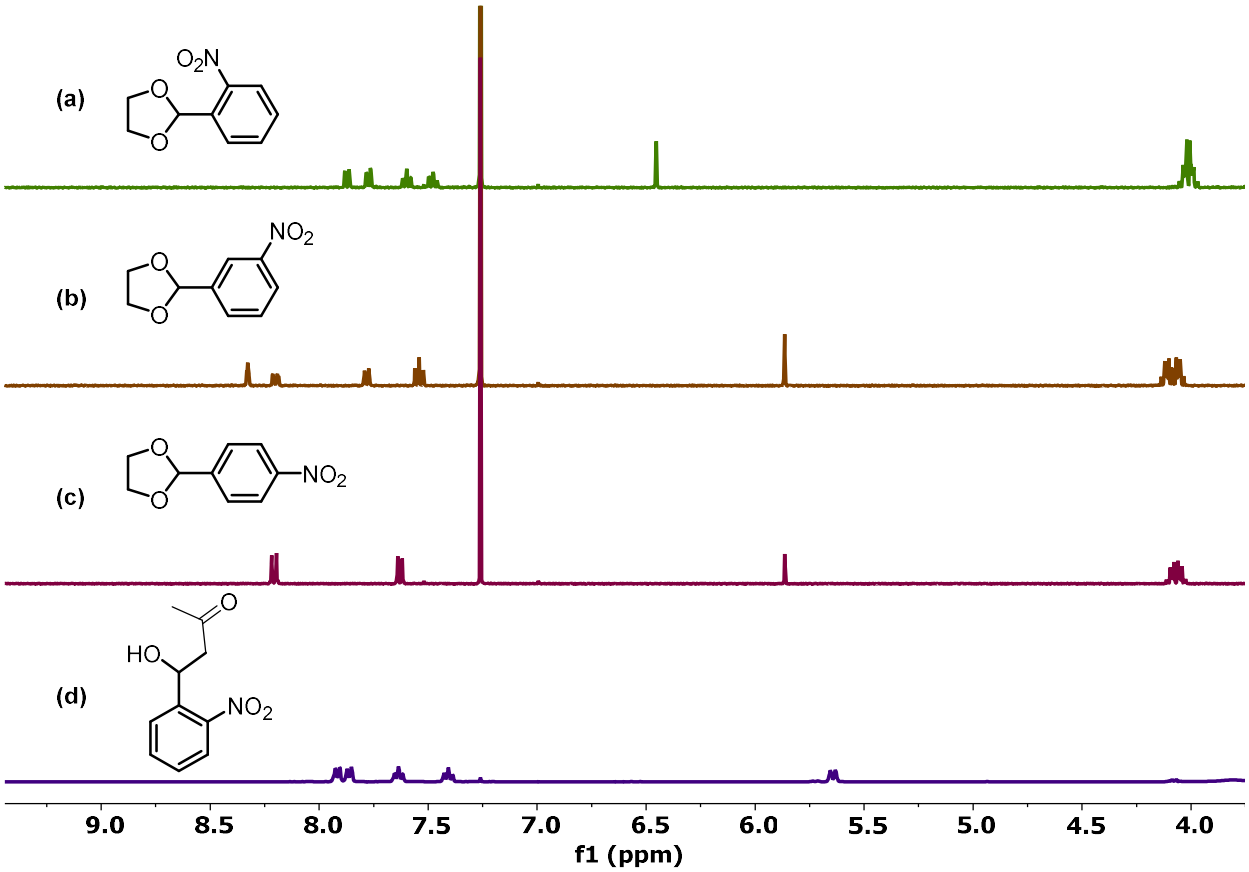

Figure S12. Partial stacked ^{1}H NMR spectra of tandem nitro aldol reaction (a) starting material **8g**, (b) starting material **8h**, (c) starting material **8i**, (d) product 4-hydroxy-4-(2-nitrophenyl)butan-2-one in $CDCl_3$.

[1]H and [13]C NMR spectra of key compounds

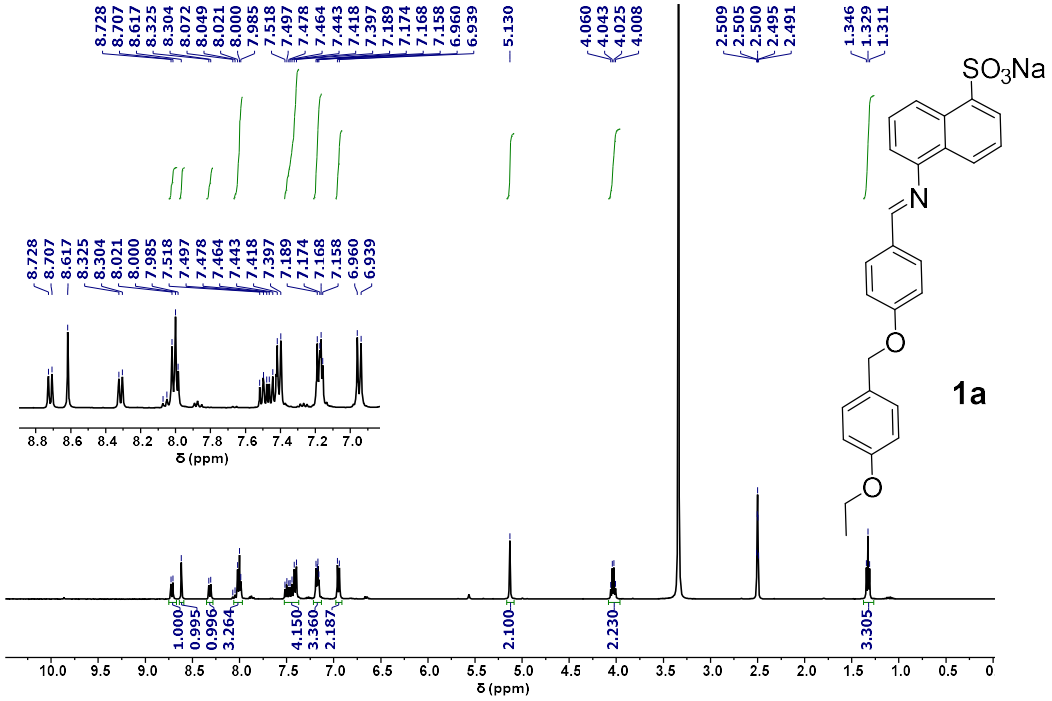

Figure S13. [1]H NMR spectrum of compound **1a**

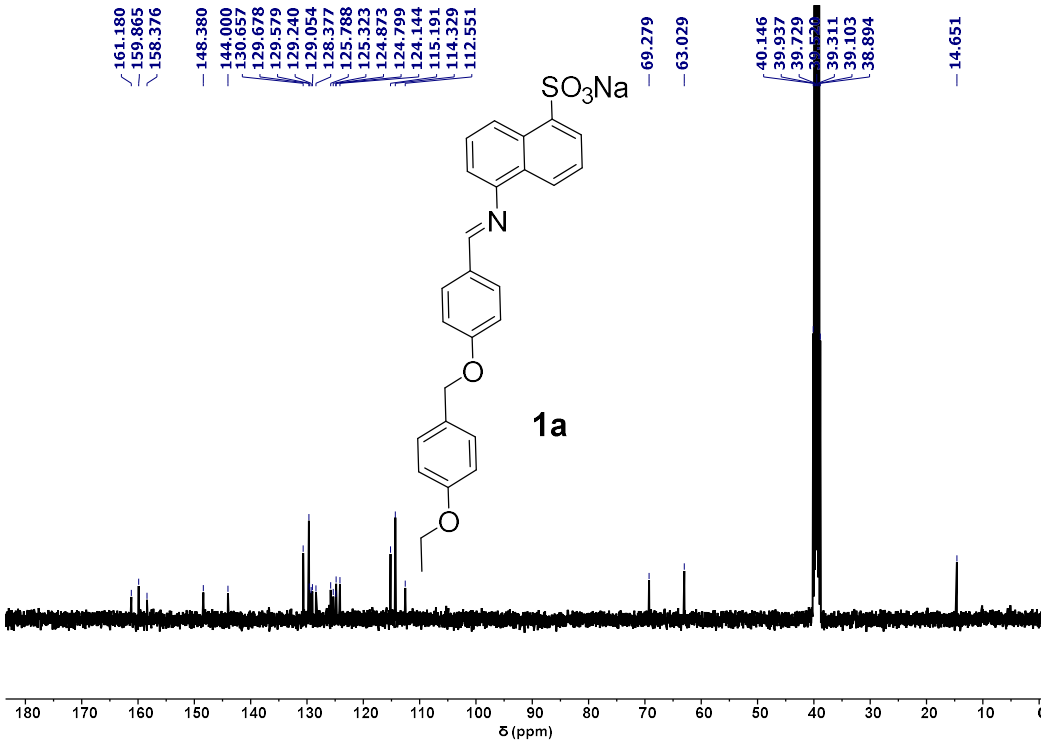

Figure S14. [13]C NMR spectrum of compound **1a**

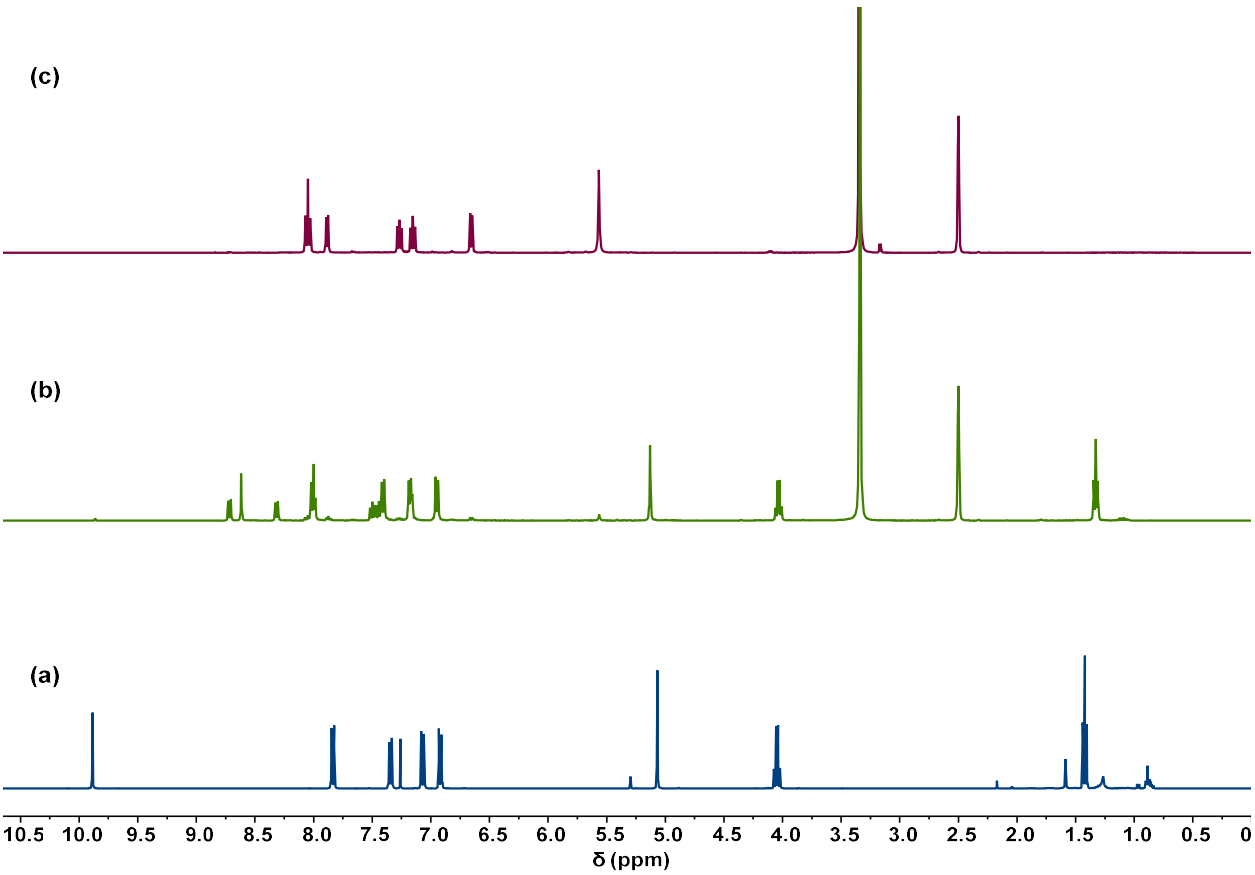

Figure S15. ^{1}H NMR spectra comparison between compounds (a) **5** in $CDCl_3$, (b) **1a** in DMSO-d_6, and (c) 5-aminonaphthalene-1-sulfonic acid in DMSO-d_6.

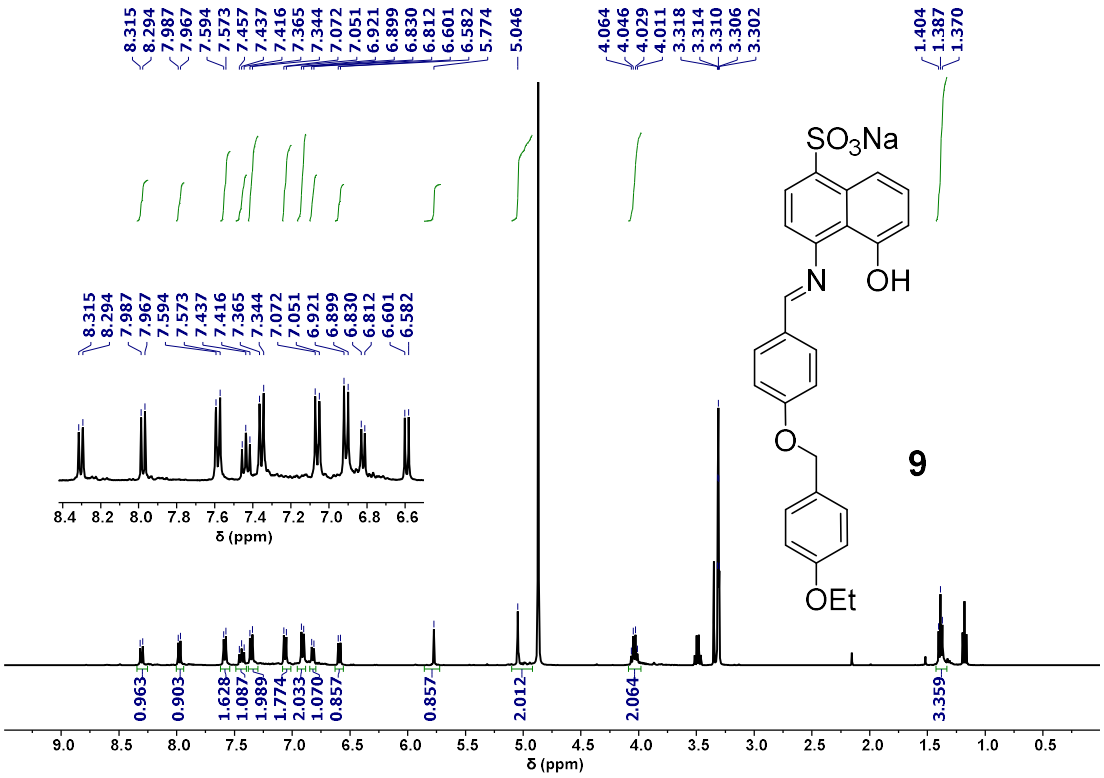

Figure S16. ^{1}H NMR spectrum of compound **9**

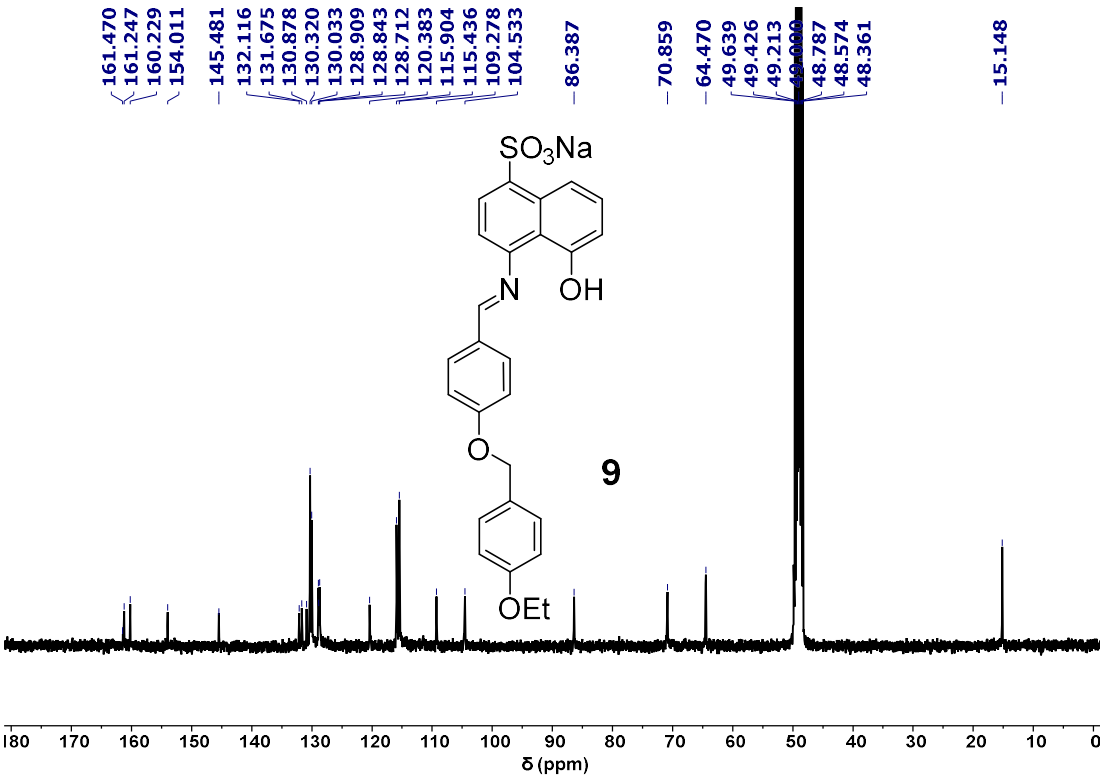

Figure S17. ^{13}C NMR spectrum of compound **9**

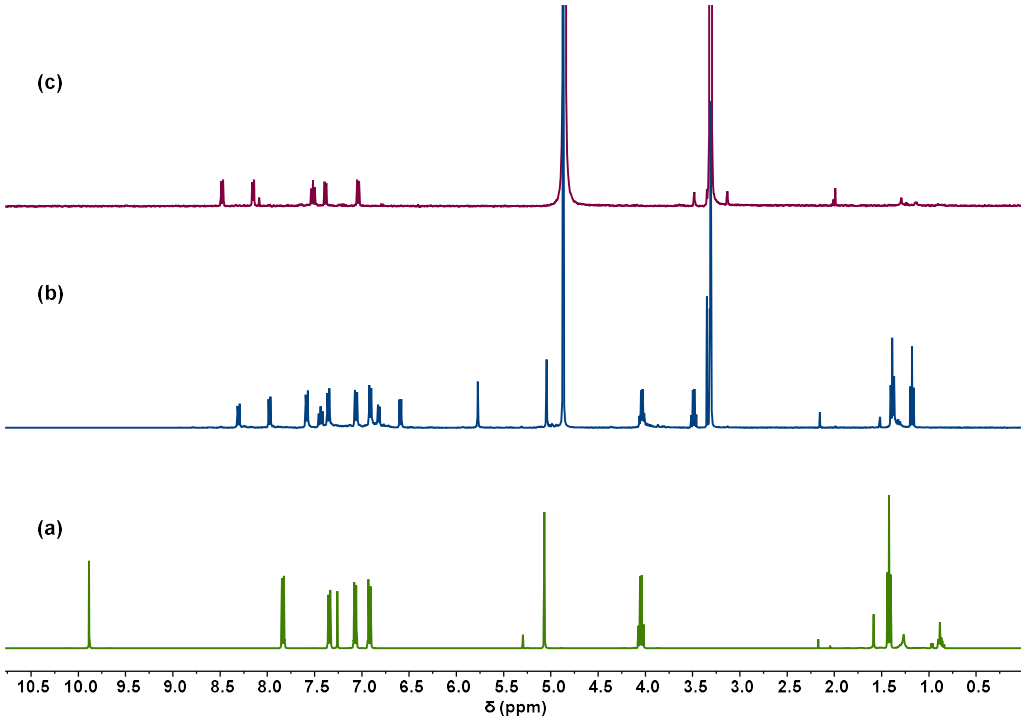

Figure S18. ^{1}H NMR spectra comparison between compounds (a) **5** in $CDCl_3$, (b) **9** in MeOD, and (c) 4-amino-5-hydroxynaphthalene-1-sulfonic acid in MeOD.

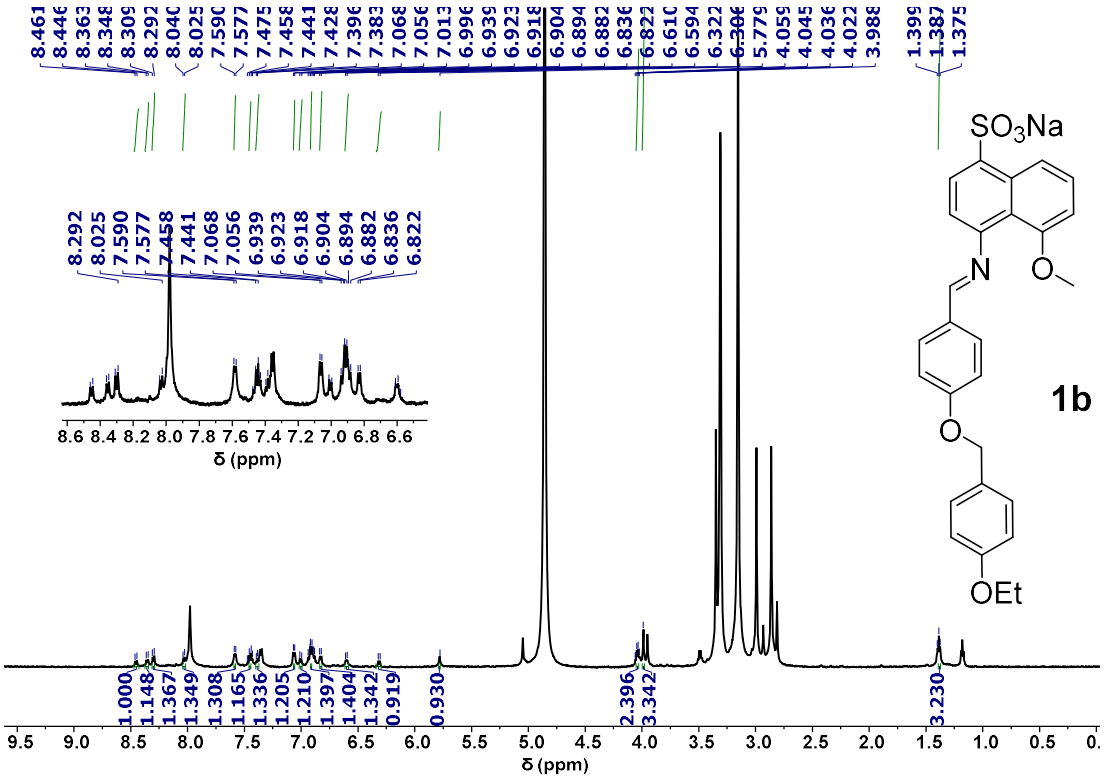

Figure S19. ^{1}H NMR spectrum of compound **1b**

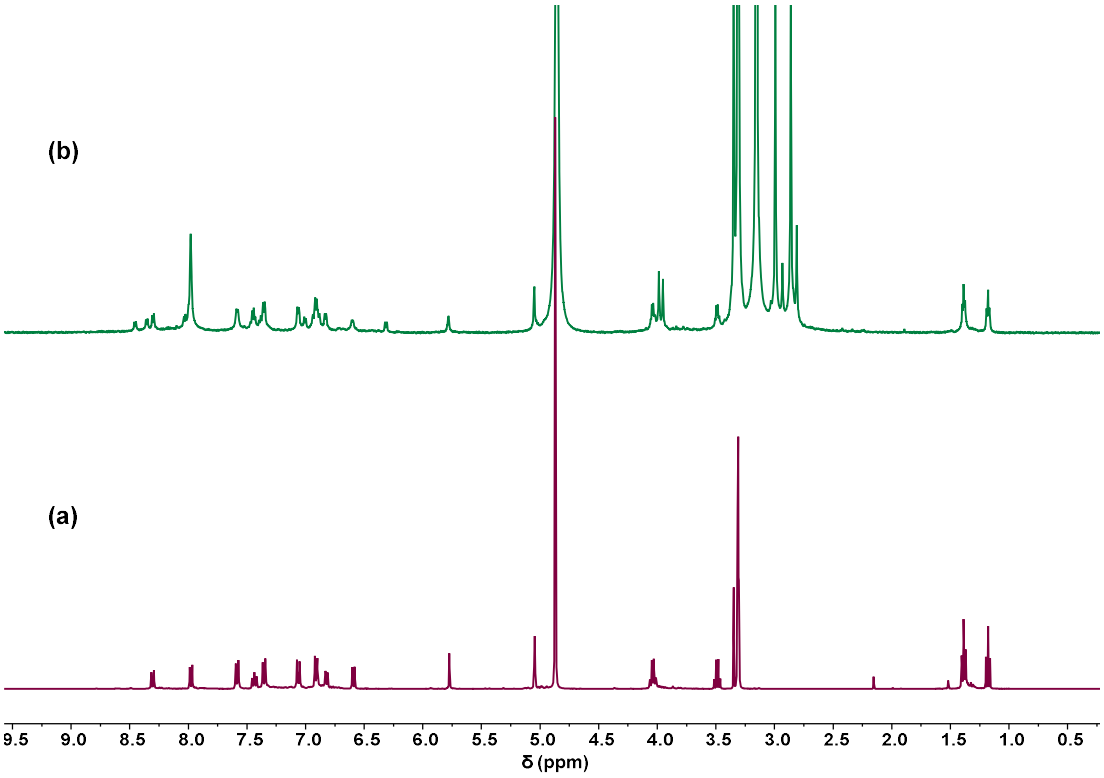

Figure S20. ^{1}H NMR spectra comparison between compounds (a) **9** in $CDCl_3$, and (b) **1b** in MeOD,.

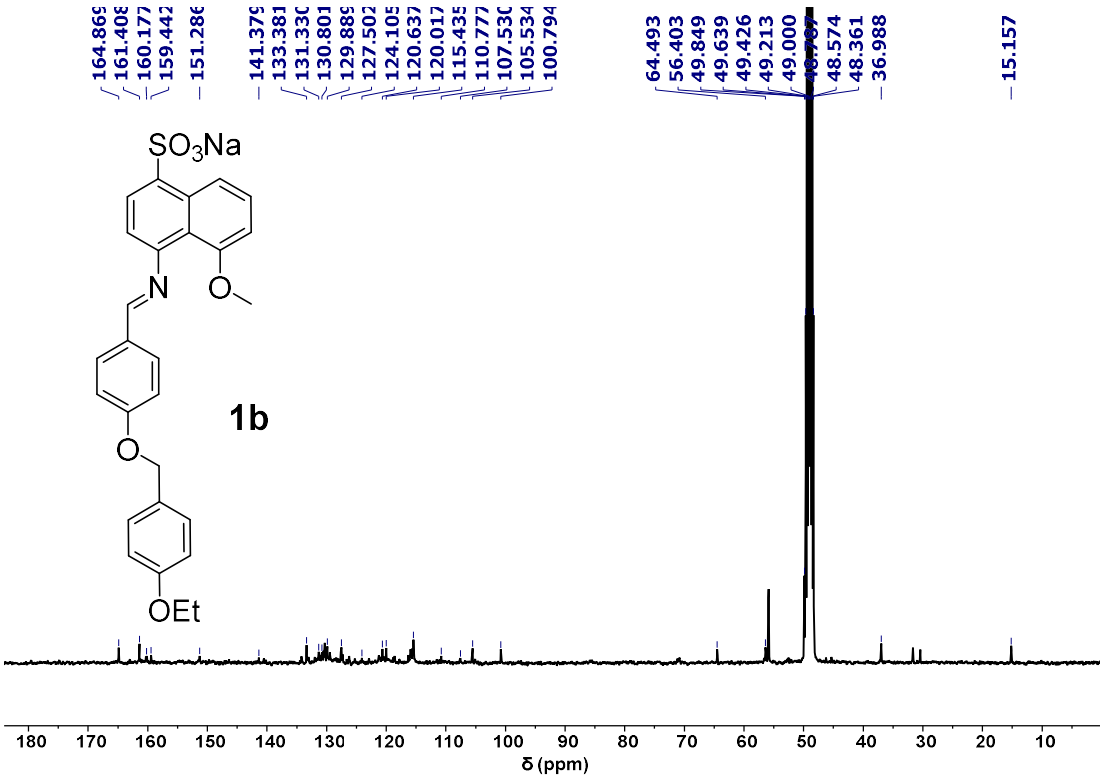

Figure S21. ^{13}C NMR spectrum of compound **1b**

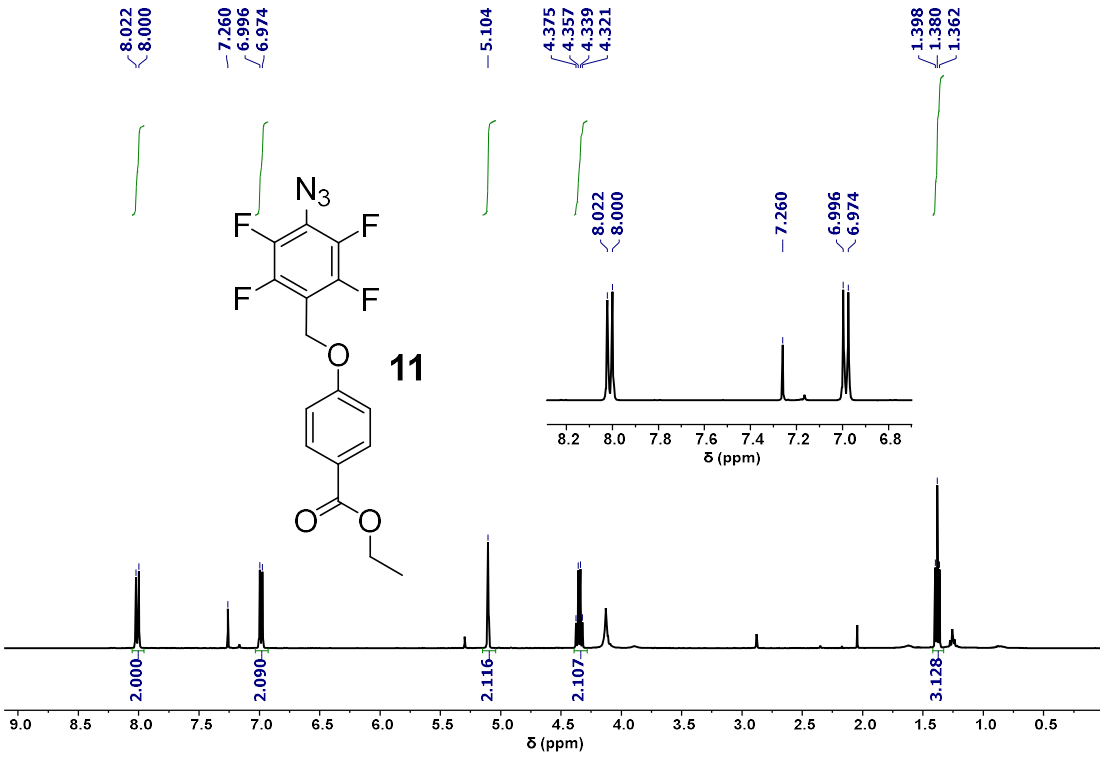

Figure S22. ^{1}H NMR spectrum of compound **11**

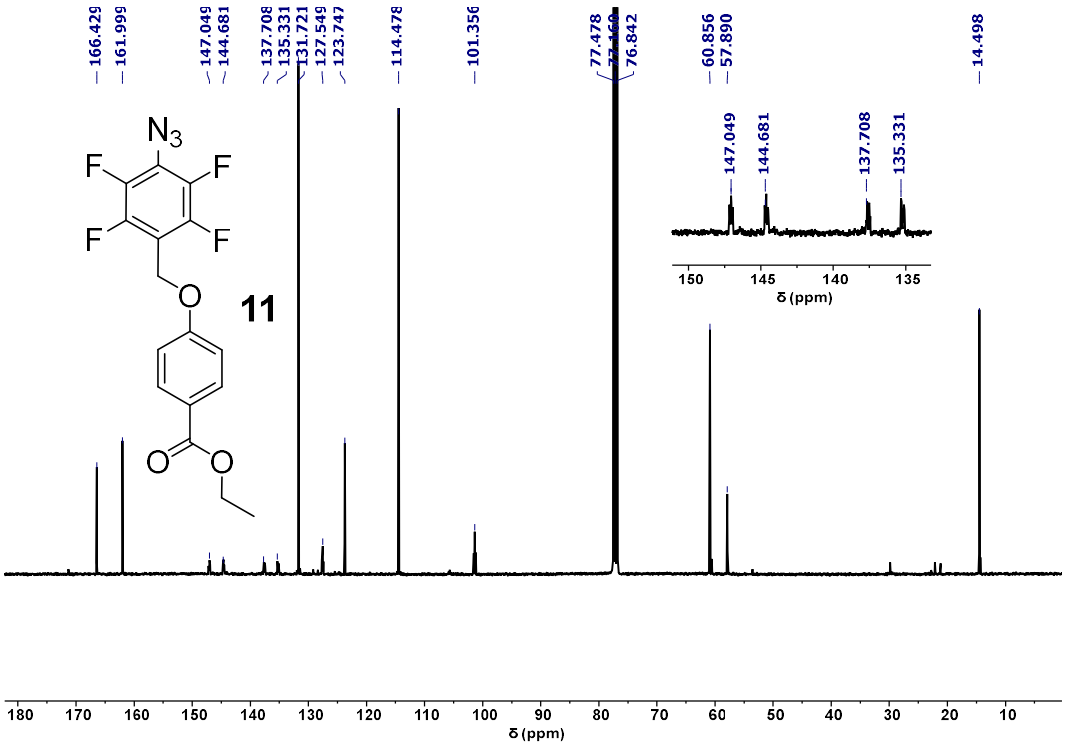

Figure S23. ^{13}C NMR spectrum of compound **11**

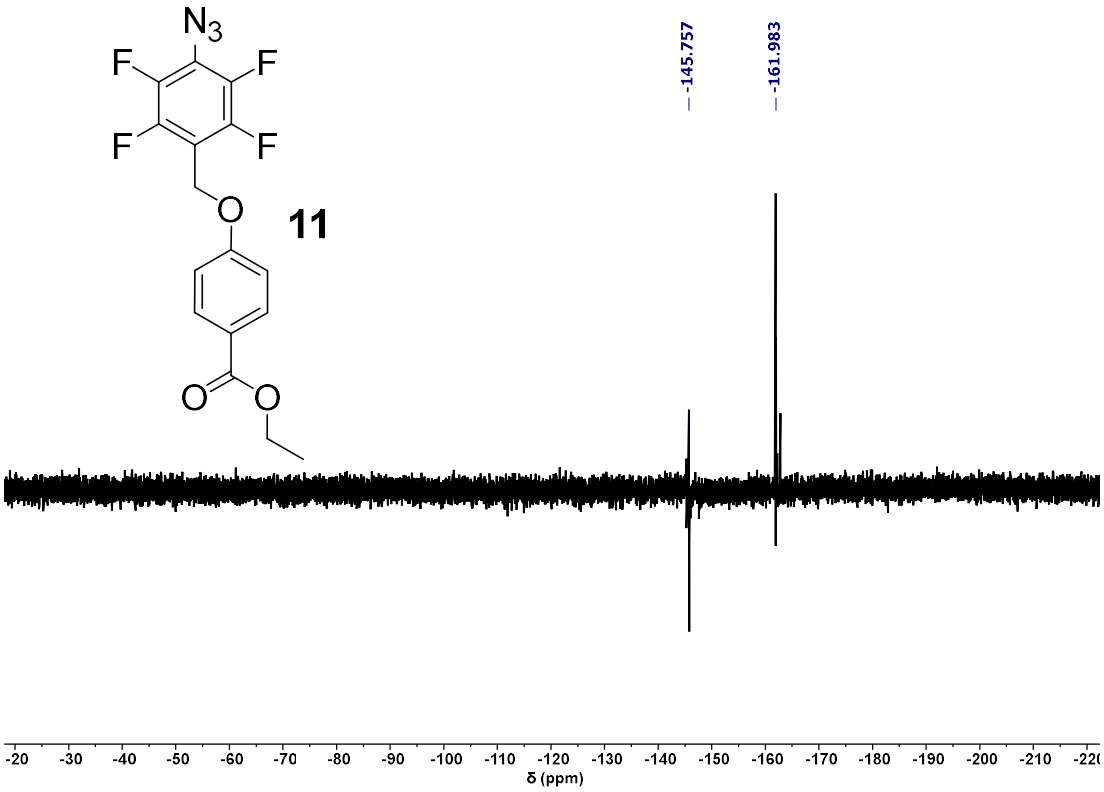

Figure S24. ^{19}F NMR spectrum of compound **11**

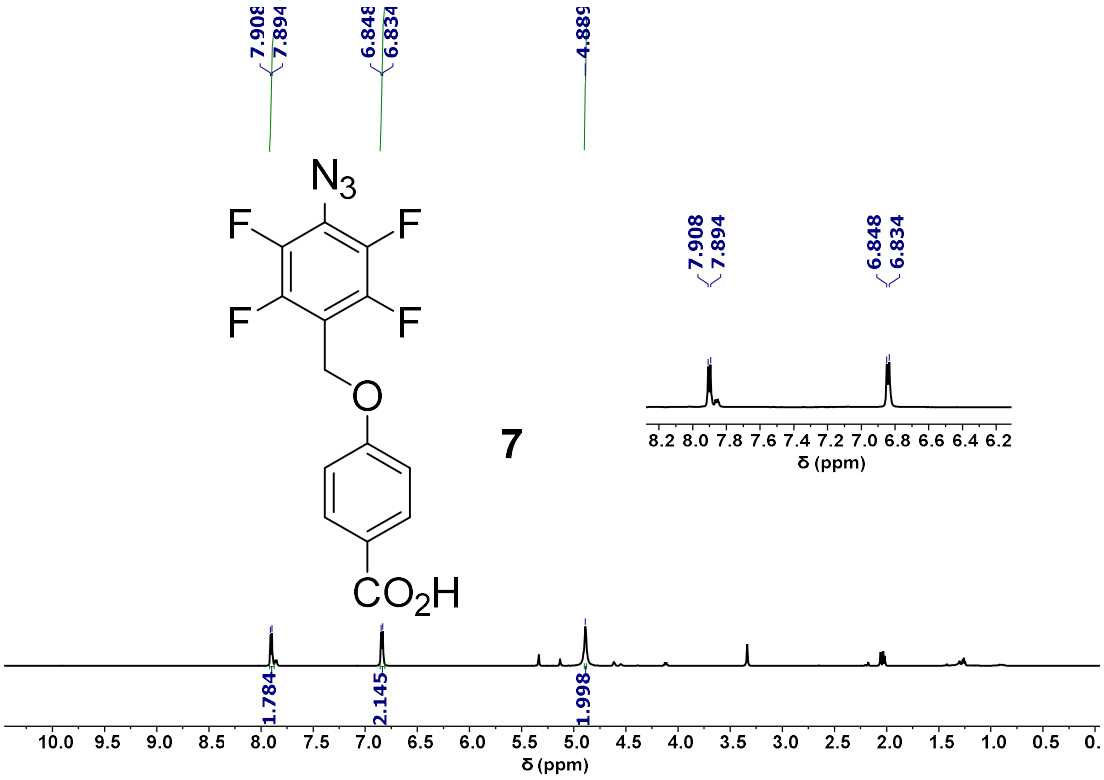

Figure S25. ^{1}H NMR spectrum of compound **7**

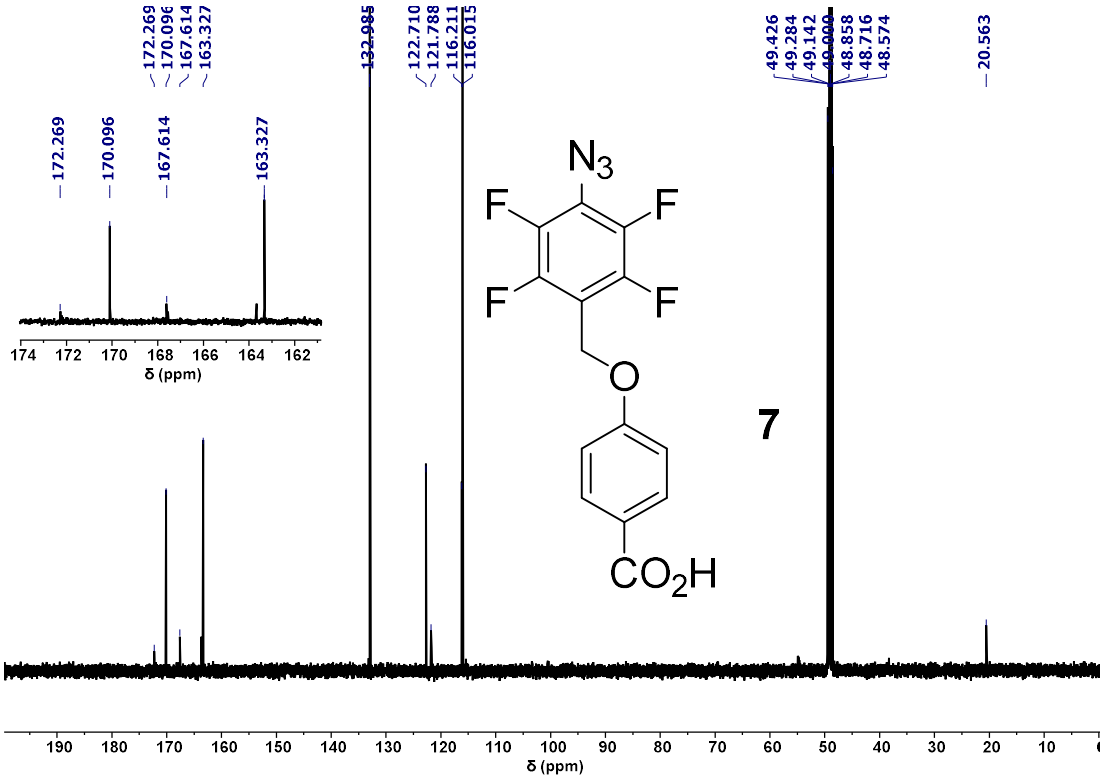

Figure S26. ^{13}C NMR spectrum of compound **7**

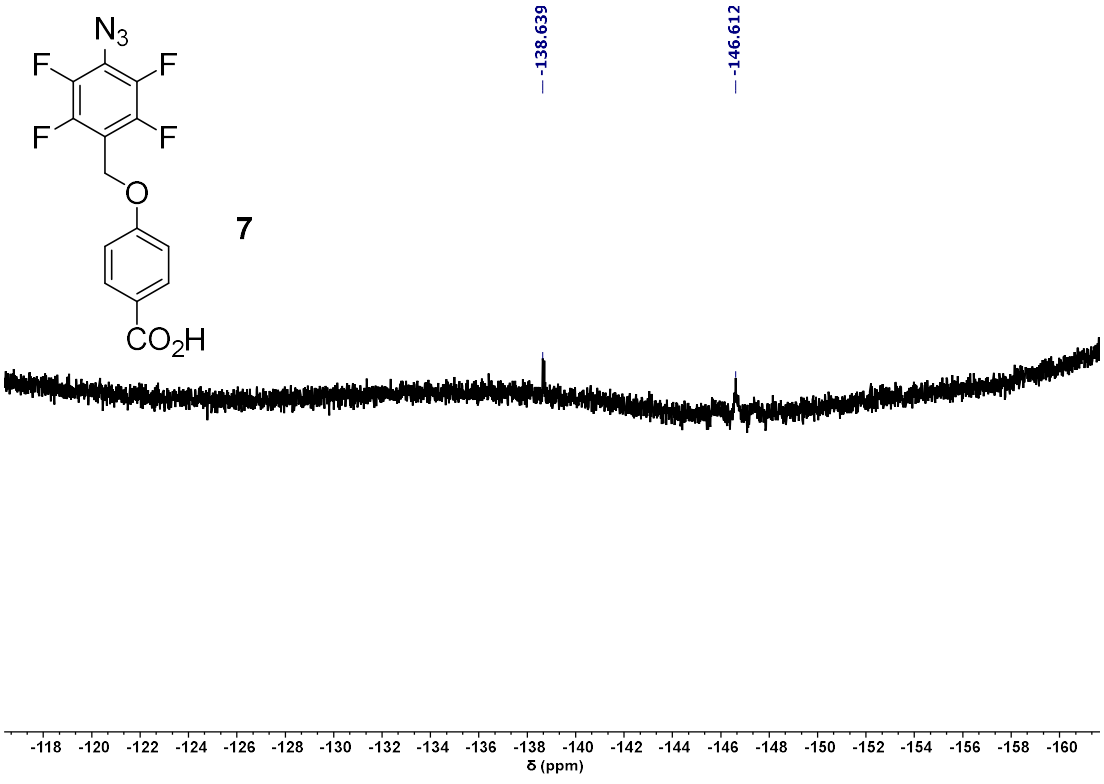

Figure S27. ^{19}F NMR spectrum of compound **7**

Mass spectra

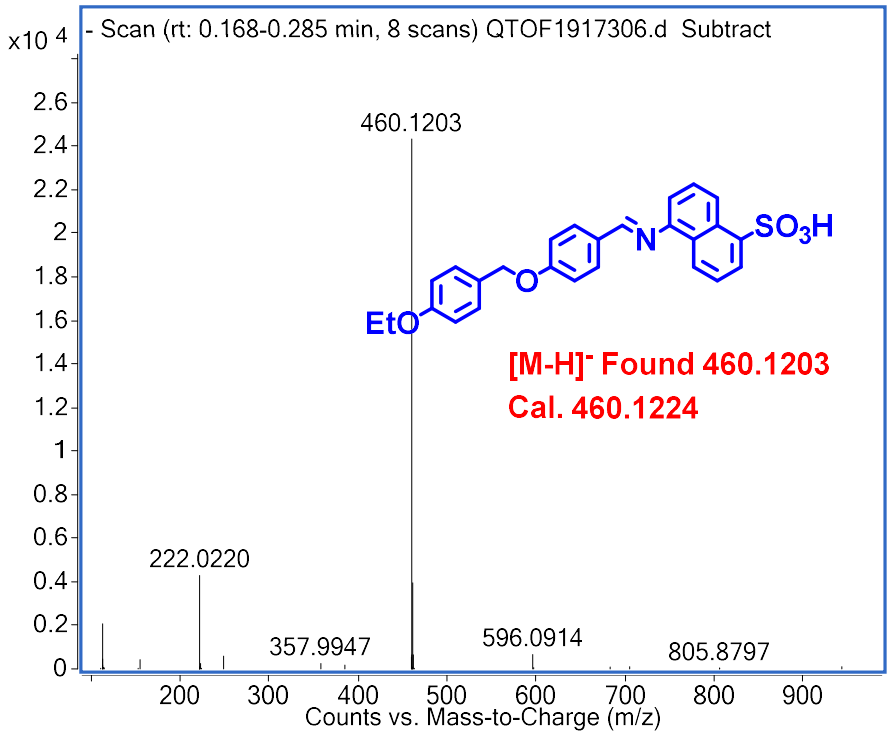

Figure S28. HRMS-ESI spectrum of compound **1a**

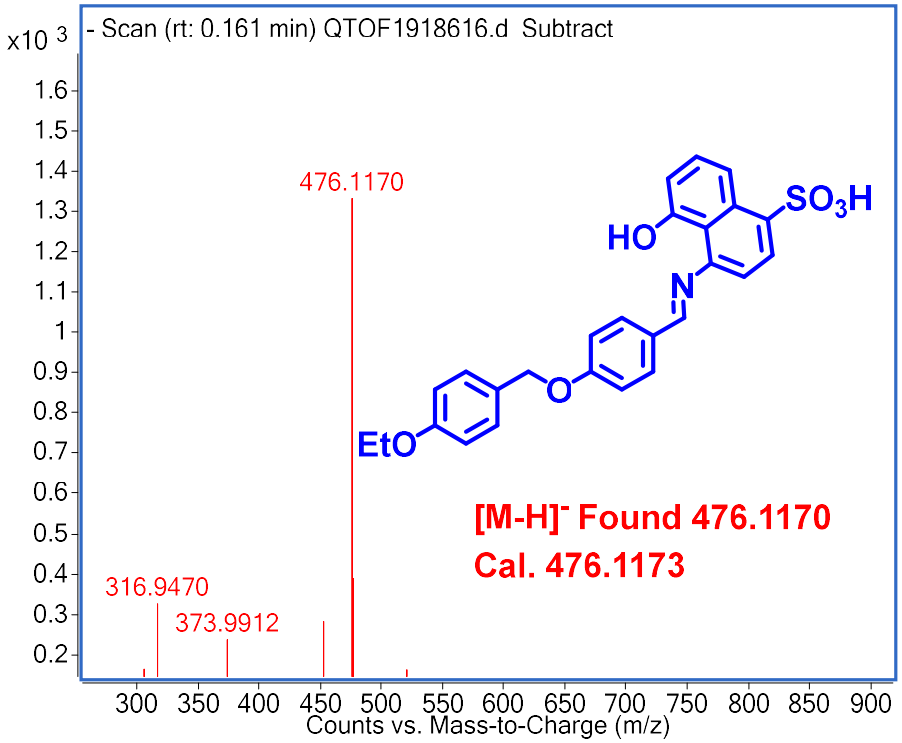

Figure S29. HRMS-ESI spectrum of compound **9**

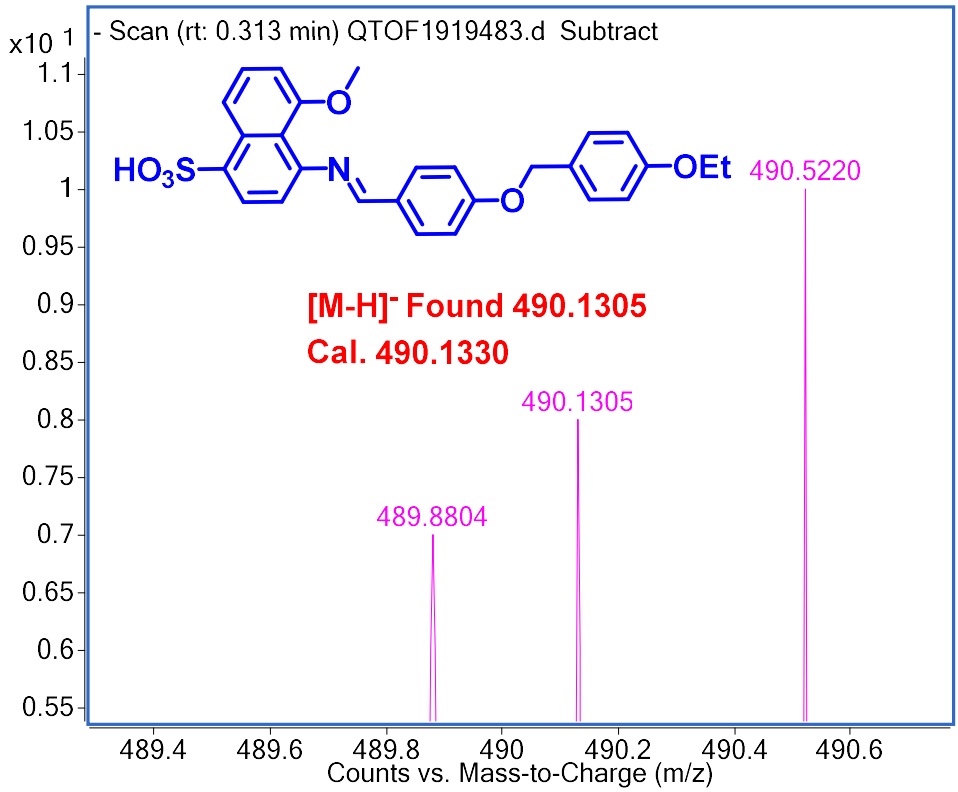

Figure S30. HRMS-ESI spectrum of compound **1b**

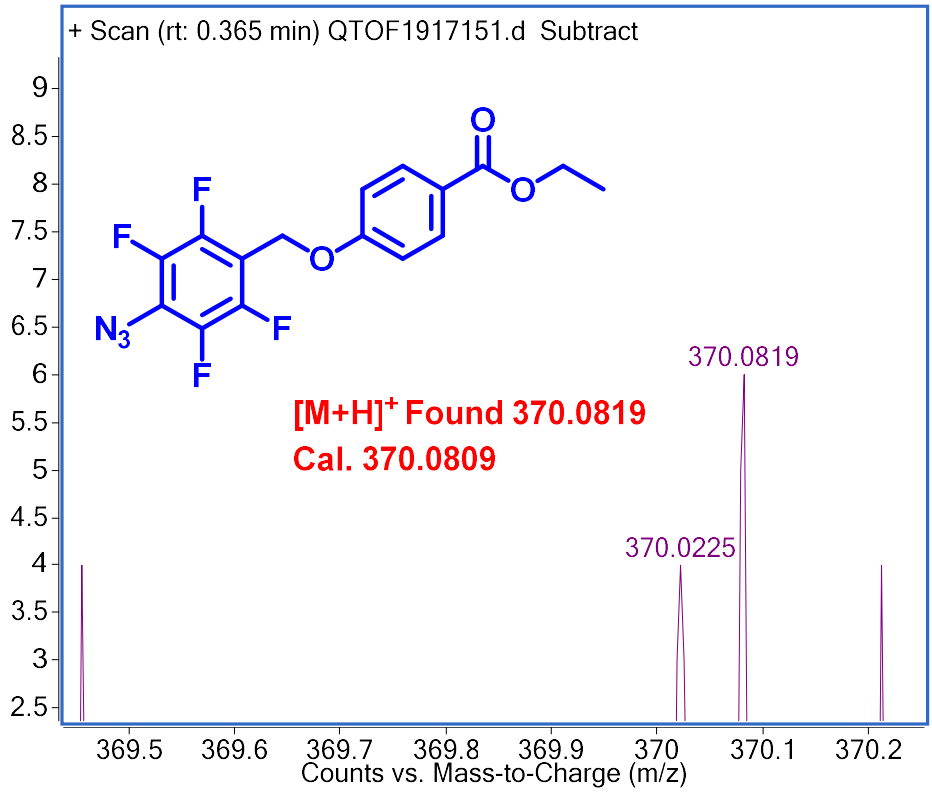

Figure S31. HRMS-ESI spectrum of compound **11**

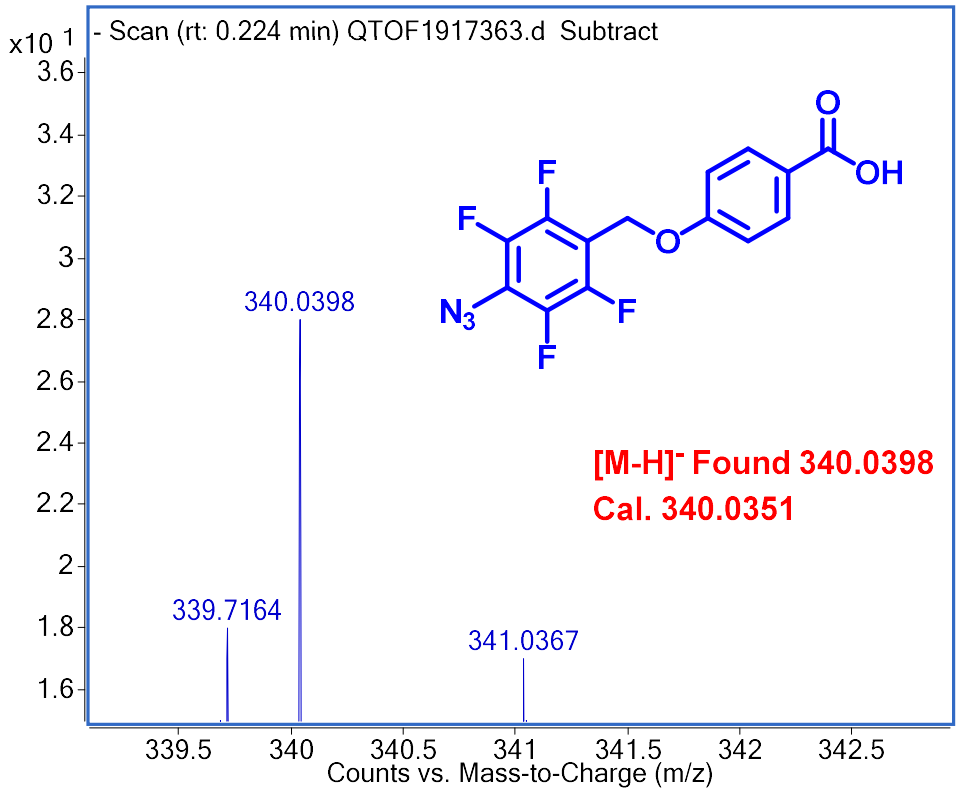

Figure S32. HRMS-ESI spectrum of compound **7**

References

1. Awino, J. K.; Zhao, Y., Protein-Mimetic, Molecularly Imprinted Nanoparticles for Selective Binding of Bile Salt Derivatives in Water. *J. Am. Chem. Soc.* **2013**, *135*, 12552-12555.

2. Zou, H.-B.; Zhang, L.; Yang, L.-X.; Yang, L.-Q.; Zhao, Y.; Yu, Y.-P.; Stöckigt, J., Synthesis and structure–activity relationship studies of cytotoxic cinnamic alcohol derivatives. *Natural Product Research* **2011**, *25*, 203-221.

3. Lv, F.; Yu, Y.; Hao, E.; Yu, C.; Wang, H.; Boens, N.; Jiao, L., Highly regioselective α-formylation and α-acylation of BODIPY dyes via tandem cross-dehydrogenative coupling with in situ deprotection. *Org. Biomol. Chem.* **2019**, *17*, 5121-5128.

4. Bose, I.; Zhao, Y., pH-Controlled Nanoparticle Catalysts for Highly Selective Tandem Henry Reaction from Mixtures. *ACS Catal.* **2020**, *10*, 13973-13977.

5. Dey, S.; Gadakh, S. K.; Sudalai, A., Titanium superoxide – a stable recyclable heterogeneous catalyst for oxidative esterification of aldehydes with alkylarenes or alcohols using TBHP as an oxidant. *Org. Biomol. Chem.* **2015**, *13*, 10631-10640.

6. Wiegand, M.; Lindhorst, T. K., Synthesis of Photoactive α-Mannosides and Mannosyl Peptides and Their Evaluation for Lectin Labeling. *Eur. J. Org. Chem.* **2006**, *2006*, 4841-4851.

7. Erickson, H. P., Size and Shape of Protein Molecules at the Nanometer Level Determined by Sedimentation, Gel Filtration, and Electron Microscopy. *Biol. Proced. Online* **2009**, *11*, 32.